Epidemics 4 (2012) 22–32

Contents lists available at SciVerse ScienceDirect

Epidemics

journal homepage: www.elsevier.com/locate/epidemics

Critical immune and vaccination thresholds for determining multiple influenza epidemic waves

Laura Matrajt[a], Ira M. Longini Jr.[b,*]

[a] Department of Medicine, University of Washington, Seattle, WA, USA
[b] Department of Biostatistics and Emerging Pathogens Institute, Colleges of Public Health and Medicine, University of Florida, Gainesville, FL, USA

ARTICLE INFO

Article history:
Received 1 August 2011
Received in revised form 2 November 2011
Accepted 29 November 2011
Available online 7 December 2011

Keywords:
Influenza
Mathematical modeling
Epidemic wave
Influenza vaccine

ABSTRACT

Previous influenza pandemics (1918, 1957, and 1968) have all had multiple waves. The 2009 pandemic influenza A (H1N1) (pandemic H1N1) started in April 2009 and was followed, in the United States (US) and temperate Northern Hemisphere, by a second wave during the fall of 2009. The ratio of susceptible and immune individuals in a population at the end of a wave determines the potential and magnitude of a subsequent wave. As influenza vaccines are not completely protective, there was a combined immunity in the population at the beginning of 2010 (due to vaccination and due to previous natural infection), and it was uncertain if this mixture of herd immunity was enough to prevent a third wave of pandemic influenza during the winter of 2010. Motivated by this problem, we developed a mathematical deterministic two-group epidemic model with vaccination and calibrated it for the 2009 pandemic H1N1. Then, applying methods from mathematical epidemiology we developed a scheme that allowed us to determine critical thresholds for vaccine-induced and natural immunity that would prevent the spread of influenza. Finally, we estimated the level of combined immunity in the US during winter 2010. Our results suggest that a third wave was unlikely if the basic reproduction number R_0 were below 1.6, plausible if the original R_0 was 1.6, and likely if the original R_0 was 1.8 or higher. Given that the estimates for the basic reproduction number for pandemic influenza place it in the range between 1.4 and 1.6 (Bacaer and Ait Dads, 2011; Fraser et al., 2009; Munayco et al., 2009; Pourbohloul et al., 2009; Tuite et al., 2010; White et al., 2009; Yang et al., 2009), our approach accurately predicted the absence of a third wave of influenza in the US during the winter of 2010. We also used this scheme to accurately predict the second wave of pandemic influenza in London and the West Midlands, UK during the fall of 2009.

Introduction

In the past century, there were three major influenza pandemics (1918, 1957, and 1968) and they all had multiple waves. There is evidence of an early wave in the spring of 1918 in the United States (US) and Europe, followed by a large wave in the fall of 1918 and a third, more mild wave, in the winter of 1919 (Olson et al., 2005; Barry et al., 2008; He et al., 2011). In the US and temperate Northern Hemisphere, 2009 influenza pandemic A (H1N1) (pandemic H1N1) started in April 2009, and it was followed by a second wave during the fall of 2009. The ratio of susceptible and immune individuals in a population at the end of a given wave, plays a crucial role in determining the possibility and magnitude of the following wave. While vaccines were not available in the previous pandemics, we now have the ability to produce vaccines quickly and in large quantities (WHO, 2009). In fact, more than 20 vaccines were developed during late spring to early summer of 2009. In several countries, vaccination started as early as mid-September and continued during the fall of 2009, so that, at the end of the second wave, a fraction of the population had acquired vaccine-induced immunity, while some fraction of the population got infected and hence acquired natural immunity. Since influenza vaccines are not completely protective, vaccine-induced immunity is not expected to be as strong as naturally acquired immunity due to natural infection. Therefore, at the end of the second wave, the population had a combination of natural and vaccine-induced immunity.

For logistical, practical, and economic reasons, estimating the number of people infected and the number of people vaccinated is not always possible. In the context of the H1N1 influenza pandemic, these estimates were extremely difficult to make. It then became important to determine if this mixture of immunity in the population was going to be enough to prevent a third wave of pandemic influenza. Motivated by this problem, we developed a simple scheme to determine the possibility of a third wave of pandemic influenza in the United States in the winter of 2010,

* Corresponding author at: Department of Biostatistics, University of Florida, 22 Buckman Drive, Gainesville, FL, 32611, USA. Tel.: +1 352 294 1938; fax: +1 352 294 1930.

1755-4365/$ – see front matter © 2011 Elsevier B.V. All rights reserved.
doi:10.1016/j.epidem.2011.11.003

based on the level of herd immunity at that time. To do this, we formulated a mathematical model for pandemic influenza. Using known techniques for computing the basic reproduction number R_0 and the effective reproduction number R_f (defined to be the reproduction number when a fraction f of the population is immune or vaccinated) we determined critical thresholds of vaccine-induced immunity and of naturally induced immunity for preventing further spread of influenza virus. By combining these thresholds we were able to obtain lower and upper bounds of the level of combined immunity in the population after the second wave of H1N1 influenza. This allowed us to correctly predict the absence of a third wave of pandemic H1N1 influenza in the US. For comparison, we investigated the occurrence of the second wave of pandemic H1N1 influenza in England during the fall of 2009, using the same scheme. This approach is easily generalizable and can be applied to other infectious diseases.

Materials and methods

Influenza has strong seasonality patterns in the temperate Northern and Southern hemispheres, usually peaking during the late fall or early winter. In other regions of the world, the peaks tend to occur during the rainy season, but the seasonality is less pronounced. The basic mechanisms for these changes are not completely understood, but there is some evidence that survival and transmission of the influenza virus are influenced by physical factors, such as humidity and temperature (Lowen et al., 2007; Schaffer et al., 1976; Shaman et al., 2010; Soebiyanto et al., 2010). In addition, influenza spreads best during periods when schools are open. The aim of our work is to predict the occurrence or absence of a new epidemic wave based on the current level of herd immunity. For this reason, we will assume, below, that we are at the beginning of the influenza season, so that, in the absence of prior immunity in the population, an epidemic wave is certain.

Mathematical model

Our influenza model is based on the standard *SIR* model, and it is an extension of the model given in (Hill and Longini, 2003). We considered a closed population of size N. Since the time scale for the spread of influenza is short compared to migration or demographics (births and deaths), none of these features are included. We divided the population into two sub-populations of children and adults of size N_1 and N_2, so that $N = N_1 + N_2$. Members in each group are either susceptibles S_{ij}, infected asymptomatic A_{ij}, infected symptomatic I_{ij}, or recovered R_{ij}, where $i = 1$ indicates children, $i = 2$ adults, while j denotes the vaccination status ($j = 0$ for the unvaccinated and $j = 1$ for the vaccinated). The following assumptions were made:

- A fraction ρ of the infected people will develop symptoms. The infected asymptomatic people never develop symptoms but are still able to transmit the infection to others. Infected asymptomatic people have their infectiousness reduced by a factor m compared to infected symptomatic people (Longini et al., 2004), where $m \in [0, 1]$.
- c_{ik} is the number of contacts per day between people in group i and people in group k, where $i, k \in \{1, 2\}$.
- p is the probability of infection given contact; it will be used here as a parameter to vary the transmissibility of the infection.
- Children and adults recover at rates γ_1 and γ_2 respectively.
- Following the ideas in (Halloran et al., 1997), we consider that vaccination has three major effects in the vaccinee, as follows
  - (i) VE_S, the vaccine efficacy for susceptibility is the ability of the vaccine to prevent infection.
  - (ii) VE_I, the vaccine efficacy for infectiousness (conditioned upon being infected) is the effect of the vaccine on reducing infectiousness.
  - (iii) VE_P, the vaccine efficacy for pathogenicity (conditioned upon being infected), accounts for the effect of the vaccine on reducing the probability of symptomatic disease given infection.

Based on these assumptions we have the following system of differential equations:

Unvaccinated	Vaccinated	
$\frac{dS_{10}}{dt} = -\lambda_1 S_{10}$	$\frac{dS_{11}}{dt} = -\lambda_1 \theta S_{11}$	(1)
$\frac{dS_{20}}{dt} = -\lambda_2 S_{20}$	$\frac{dS_{21}}{dt} = -\lambda_2 \theta S_{21}$	(2)
$\frac{dA_{10}}{dt} = \lambda_1(1-\rho) S_{10} - \gamma_1 A_{10}$	$\frac{dA_{11}}{dt} = \lambda_1(1-\rho\psi)\theta S_{11} - \gamma_1 A_{11}$	(3)
$\frac{dA_{20}}{dt} = \lambda_2(1-\rho) S_{20} - \gamma_2 A_{20}$	$\frac{dA_{21}}{dt} = \lambda_2(1-\rho\psi)\theta S_{21} - \gamma_2 A_{21}$	(4)
$\frac{dI_{10}}{dt} = \lambda_1 \rho S_{10} - \gamma_1 I_{10}$	$\frac{dI_{11}}{dt} = \lambda_1 \rho\psi\theta S_{11} - \gamma_1 I_{11}$	(5)
$\frac{dI_{20}}{dt} = \lambda_2 \rho S_{20} - \gamma_2 I_{20}$	$\frac{dI_{21}}{dt} = \lambda_2 \rho\psi\theta S_{21} - \gamma_2 I_{21}$	(6)
$\frac{dR_{10}}{dt} = \gamma_1(A_{10} + I_{10})$	$\frac{dR_{11}}{dt} = \gamma_1(A_{11} + I_{11})$	(7)
$\frac{dR_{20}}{dt} = \gamma_2(A_{20} + I_{20})$	$\frac{dR_{21}}{dt} = \gamma_2(A_{21} + I_{21})$	(8)

where $VE_S = 1 - \theta$, $VE_I = 1 - \phi$ and $VE_P = 1 - \psi$. The forces of infection for children and adults, respectively, are given by

$$\lambda_1 = \frac{pc_{11}}{N_1}(mA_{10} + m\phi A_{11} + I_{10} + \phi I_{11}) + \frac{pc_{12}}{N_2}(mA_{20} + m\phi A_{21} + I_{20} + \phi I_{21}) \quad (9)$$

and

$$\lambda_2 = \frac{pc_{21}}{N_1}(mA_{10} + m\phi A_{11} + I_{10} + \phi I_{11}) + \frac{pc_{22}}{N_2}(mA_{20} + m\phi A_{21} + I_{20} + \phi I_{21}). \quad (10)$$

Computation of the basic reproduction number

In this section we follow the ideas of Hill and Longini (2003) and Longini et al. (1998). Let f_1 be the fraction of vaccinated children and f_2 be the fraction of vaccinated adults, where we assume that vaccination occurred before the (possible) epidemic.

The basic reproduction number R_0 for a given disease is defined as the expected number of secondary infections resulting from a single typical infectious person in a completely susceptible population, and R_f is defined to be the effective reproduction number, which is the reproduction number in the presence of vaccination. We use the approach given in Diekmann et al. (1990), Brauer et al. (2008), and van den Driessche and Watmough (2002) to compute the next generation matrix K and effective reproduction number R_f. The details of this computation can be found in Appendix A.

If $R_f > 1$, the epidemic will grow, whereas if $R_f \leq 1$, the epidemic will die out (Diekmann et al., 1990). We set $R_f = 1$ as the threshold of interest. We note that if $f_1 = f_2 = 0$, then no vaccination occurred, and the effective reproduction number is in fact the basic reproduction number, R_0.

We assume natural infection confers complete protection against reinfection, equivalent to setting $\theta = 0$ in the vaccinated Eqs. (1) and (2). So, to model the fraction of children and adults who previously got the infection and who are now immune, we simply set $\theta = 0$ in our computations. We let R_n be the effective reproduction number with natural immunity, that is, the effective reproduction number when a fraction of the population has natural immunity ($\theta = 0$).

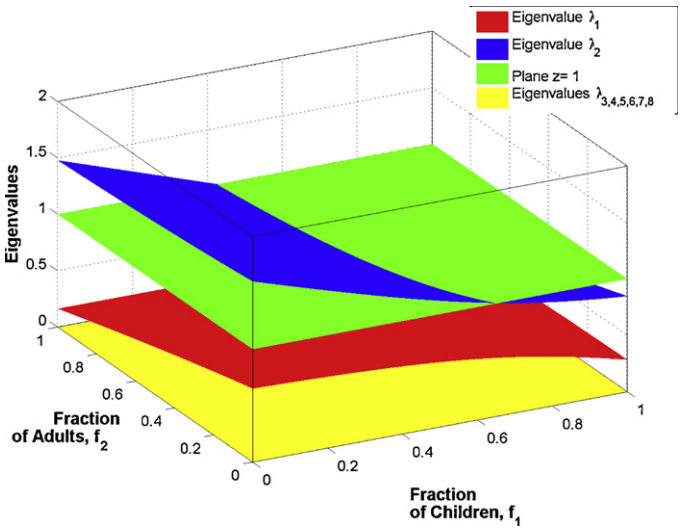

Fig. 1. Surfaces representing all the eigenvalues of the next generation matrix for $R_0 = 1.6$. All the eigenvalues of the matrix but two are zero (plotted in yellow). The ones that are non-zero are plotted above in red and blue. The green plot corresponds to the plane $z = 1$. Here, the blue surface corresponds to the effective reproduction number with vaccination, $R_f(f_1, f_2)$. (For interpretation of the references to color in this figure legend, the reader is referred to the web version of this article.)

Scheme to determine the possibility of multiple epidemic waves

In this section, we outline the scheme we developed to investigate the possibility of multiple influenza epidemic waves using the model and the thresholds established above. In the next section, we will use this approach to predict the absence of a third wave of pandemic H1N1 influenza in the United States during the winter of 2010.

We begin by noting that if all the parameters of the model are known except for the values of f_1 and f_2, then R_f becomes a function of f_1 and f_2. We define $R_f(f_1, f_2)$ as the effective reproduction number with a fraction f_1 of vaccinated children and a fraction f_2 of vaccinated adults. Analogously, $R_n(f_1, f_2)$ is the effective reproduction number with f_1 of the children and f_2 of the adults completely immune (due to previous infection). The threshold condition is then equivalent to finding the contour lines in the $f_1 f_2$-plane where $R_f(f_1, f_2) = 1$. For all the points above the curve $\Gamma = \{f = (f_1, f_2) \mid R_f(f_1, f_2) = 1\}$, $R_f < 1$ and the epidemic will not occur, while for points below the curve Γ, $R_f > 1$ and the epidemic will occur. While these curves may not be unique, they separate the $f_1 f_2$-plane into connected regions where either $R_f < 1$ or $R_f > 1$.

We define a critical vaccination vector to be a pair (f_1, f_2) such that $R_f(f_1, f_2) = 1$. Analogously, we define a critical immune vector to be a pair (f_1, f_2) such that $R_n(f_1, f_2) = 1$. The critical vaccination vector gives us a pair of fractions of each subpopulation that should be vaccinated such that no significant transmission can occur. In addition, the critical immune vector gives us a pair of those fractions of each subgroup that must be completely immune for no transmission to occur in the entire population.

In general, finding an analytical solution for the contour lines of $R_f(f_1, f_2) = 1$ is difficult, since we need to find the roots of a polynomial of degree eight. To overcome this problem, we use symbolic or numeric software to compute the values of all the eigenvalues of the next generation matrix K as a function of f_1 and f_2. In this fashion, we obtain surfaces representing all the different eigenvalues. An example is given in Fig. 1. Plotting the surfaces can be helpful when a closed analytical form of the eigenvalues is not available, since this allows us to determine which eigenvalue has the largest absolute value. We then intersect the largest surface (corresponding to the largest eigenvalue) with the plane $\mathcal{P} = \{z = 1\}$. We graph the contour lines of R_f and R_n for which $R_f(f_1, f_2) = 1$ and $R_n(f_1, f_2) = 1$ are satisfied, and by doing so we determine the critical vaccination vectors and the critical immune vectors. If the structure of the problem allows it, one can find explicit analytic solutions for the eigenvalues of the matrix K, and hence explicitly compute the contour lines. Once we have determined a way to compute these contour lines, the analysis is carried out in three steps.

First, we assume that the only way to be protected just before the start of a new influenza season is to be vaccinated. We then compute the critical vaccination vectors using the method described above. In this fashion we obtain thresholds for the fraction of vaccinated children and adults needed to prevent a further epidemic wave. While this is not realistic, since people who got influenza in a previous wave would have some degree of protection, it permits us to isolate the effects of vaccination from those of natural immunity at the population level.

Second, we assume that the only way to be protected just before the start of a new influenza season is to be naturally immune, that is, to have acquired the infection in a previous wave. This scenario will only be realistic if a vaccine for the particular influenza strain did not exist, but, as before, it allows us to separate out the effects of natural immunity. We then compute the critical immune vectors, providing us with a threshold for the fraction of naturally immune children and adults needed to prevent a further epidemic.

Finally, we combine this information to establish upper and lower bounds for the threshold on the fractions of children and adults, either vaccinated or naturally immune, that would prevent a new wave of influenza. In this way, we predict the regions in the $f_1 f_2$−plane that would result in a third wave and the regions in the plane that would prevent a third wave. We then compute estimates of the number of children and adults infected and vaccinated, and compare these estimates with our thresholds. If the estimates lie above the thresholds, there is sufficient combined herd immunity to prevent a subsequent epidemic wave. If the estimates lie below the threshold, a new epidemic wave is possible. If the estimate lies between the lower and upper bound, then the method is inconclusive. This approach will be clarified in the next section, when we use it to predict the absence of a third wave of pandemic influenza in the United States during the winter 2009–2010, and to predict the occurrence of the second wave of pandemic influenza in England during the fall 2009.

Application: 2009 pandemic H1N1 influenza

Third wave in the United States

During the first (Spring 2009) and second (Fall 2009) waves of the pandemic H1N1, a significant fraction of the population got infected and became naturally immune. Meanwhile, several vaccines were developed and during the second wave, a fraction of children and adults got vaccinated. We used the model and approach described above to accurately predict the absence of a third wave of pandemic influenza in the United States during the winter of 2010.

Model calibration

Based on current estimates (e.g. Balcan et al., 2009; Bacaer and Ait Dads, 2011; Fraser et al., 2009; Munayco et al., 2009; Pourbohloul et al., 2009; Tuite et al., 2010; White et al., 2009; Yang et al., 2009), we considered R_0 for pandemic H1N1 to lie in the interval [1.2, 1.8]. We used the parameter p to vary the intensity of the infection by selecting values of p for which the original basic reproduction number would be in the range [1.2, 1.8]. We calibrated the model (1)–(8) for the pandemic H1N1 epidemic in the US according to Table 2. Using Hill and Longini (2003) as a guide, we manually

Table 1
Contact matrix.

	Children	Adults
Children	1	0.2
Adults	0.2	0.4

computed the contact rates c_{ij} given in Table 1 so that the final illness attack rates (defined as the percentage of the population that became ill with influenza) shown in Table 3 would match the final illness attack rates observed at the end of the second wave of pandemic influenza in the United States (Centers for Disease Control and Prevention, 2010a). These numbers satisfy the following three conditions: first, the number of contacts within the child group is higher than the contacts between children and adults and within the adult group. Secondly, the number of contacts in the diagonal (child-to-child and adult-to-adult) is higher than the off-diagonal contacts. This is in agreement with previously published contact studies (Wallinga et al., 2006; Mossong et al., 2008). Finally, the ratio of the illness attack rate in children to adults is similar to the one obtained from the CDC estimates (Centers for Disease Control and Prevention, 2010a). We further assumed symmetry in the contacts, i.e. $c_{ij} = c_{ji}$. While we acknowledge that this is a limitation of our model, we performed a thorough sensitivity analysis in these parameters as shown below.

The numbers of previously infected or vaccinated people are used in our scheme to compute the effective reproductive number. For this reason, we need to take into account all the people who became previously infected or were vaccinated against this particular strain of influenza. This implies that we need to consider the number of infected (or vaccinated) people that resulted from both the first and the second waves of pandemic H1N1 in 2009. The estimates for the final attack rates provided by the CDC are the cumulative numbers for the total number of people vaccinated and infected up to December 2009. This implies that these estimates combine the attack rates of the first and the second wave of pandemic H1N1, giving us the desired estimates.

We assumed that pandemic H1N1 vaccines have similar efficacies to the ones for seasonal vaccines, and hence we took the vaccine efficacies for susceptibility, infectiousness and pathogenicity as an average between well-matched live attenuated vaccine and a well-matched inactivated vaccine using the estimates given in Basta et al. (2008).

Finding the eigenvalue surfaces

For each R_0 in the range given above, we used symbolic software (Mathematica) to obtain surfaces of the eigenvalues of the next generation matrix K as described in the previous section. Here, the structure of our model resulted in a next generation matrix of rank 2. This implies that zero is an eigenvalue of multiplicity 6 and we were able to compute closed analytic formulas for the two non-zero eigenvalues. The explicit formulas can be found in Appendix A.

Recall that this analysis is done in three steps. First, we assume that the only way to be protected at the beginning of the influenza season is by being vaccinated. For instance, Fig. 1 shows all the eigenvalue surfaces in the presence of vaccination together with the plane $\mathcal{P} = \{z = 1\}$ and $R_0 = 1.6$. We determine the spectral radius of this matrix $R_f(f_1, f_2)$, as the largest of these surfaces, and numerically compute the contour lines for which $R_f(f_1, f_2) = 1$. These contour lines are shown in Fig. 2. We will refer to these lines as the critical vaccination curves. The points above this curve (the green region in Fig. 2) correspond to coverages of a vaccinated fraction f_1 of children and a vaccinated fraction f_2 of adults that will make the effective reproduction number be below one, so that no further transmission of the infection would be possible. For example, if 60% of the children and 10% of the adults were vaccinated during the second wave, that would be enough to prevent a new epidemic wave. This would also be true if 45% of the children and 75% of the adults were vaccinated.

Then, we repeated this analysis to find the critical immune curves (here $\theta = 0$). Under this scenario, the only way to be protected at the beginning of the influenza season is by being naturally immune. An example of the critical immune curves for $R_0 = 1.6$, is given in Fig. 3. For example, once 45% or more of children coupled with 10% or more of adults have already been infected, there would be no chance of transmission; or if 33% or more of children immune coupled with 75% or more of adults have previously been infected it would have the same effect.

Since influenza vaccines are not completely protective, the critical vaccination curves will always lie above the critical immune curves. The threshold curve for a mixture of vaccination-induced

Table 2
Parameter values.

Parameter	Description	Value	Reference
γ_1	Recovery rate for children	0.449	Longini et al. (1978)[a]
γ_2	Recovery rate for adults	0.329	Longini et al. (1978)[b]
ρ	Fraction of symptomatic	2/3	Longini et al. (2004) and Carrat et al. (2008)
m	Reduction of infectiousness for asymptomatics	0.5	Longini et al. (2004) and Ciofi degli Atti et al. (2008)
$c_{11}, c_{12}, c_{21}, c_{22}$	Contact rates	1,0.2, 0.2, 0.4	Calculated[c]
VE_S, VE_I, VE_P	Vaccine efficacies for susceptibility, infectiousness and pathogenicity	0.4, 0.45, 0.75	Basta et al. (2008)
N	Total population	200,000	Assumption
	Initially infected fraction of the population	1	Assumption
	Percentage of children under 18 (US)	24.16	US Census Bureau (2009)

[a] Computed as a weighted average from the rates given by Longini et al. (1978).
[b] Computed as a weighted average from the rates given by Longini et al. (1978).
[c] The contact rates were calculated to obtain the final illness attack rates shown in Table 3.

Table 3
Final illness attack rates for the range of basic reproduction numbers considered.

Value of p used	R_0	Overall illness attack rate	Illness attack rate in children (%)	Illness attack rate in adults (%)
0.5885	1.2	12.2	21.4	9.3
0.6868	1.4	23.6	36.9	19.4[a]
0.7850	1.6	31.8	45.9	27.3
0.8830	1.8	38.2	51.8	33.9

[a] These final attack rates approximately match the attack rates published by Centers for Disease Control and Prevention (2010a)

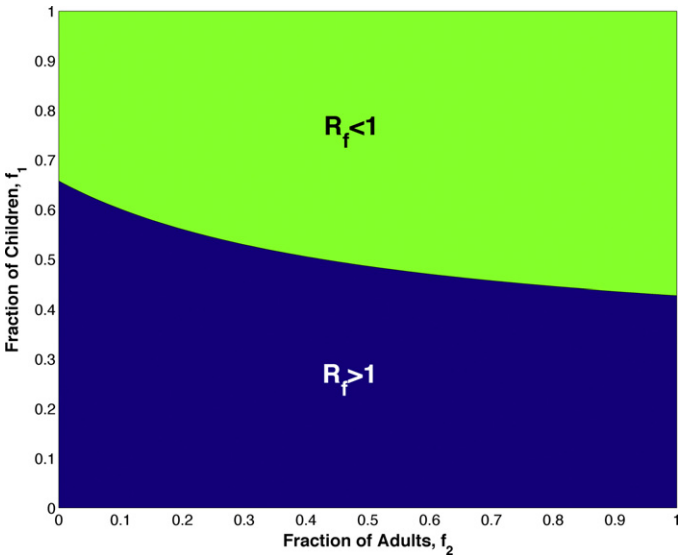

Fig. 2. Contour curve for $R_f(f_1, f_2) = 1$. The points (f_1, f_2) on the curve are the critical vaccination vectors.

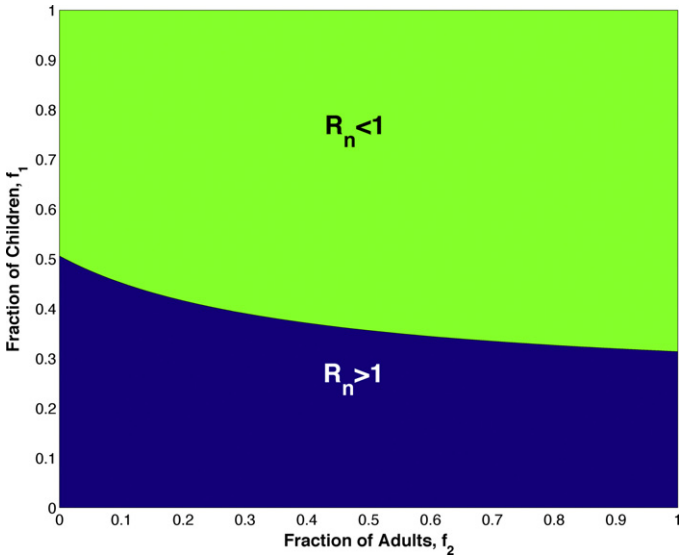

Fig. 3. Contour curve for $R_n(f_1, f_2) = 1$. The points (f_1, f_2) on the curve are the critical immune vectors.

immunity and natural immunity should then lie somewhere between the critical vaccination curve and the critical immune curve. We call this region the *intermediate region*. Fig. 4 shows the intermediate regions for several basic reproduction numbers.

Estimating our level of combined protection in winter 2010

Suppose that we know that exactly $x\%$ of the children got infected during the previous wave and exactly $y\%$ of the children got vaccinated, then, ideally, $(x+y)\%$ of the children would be

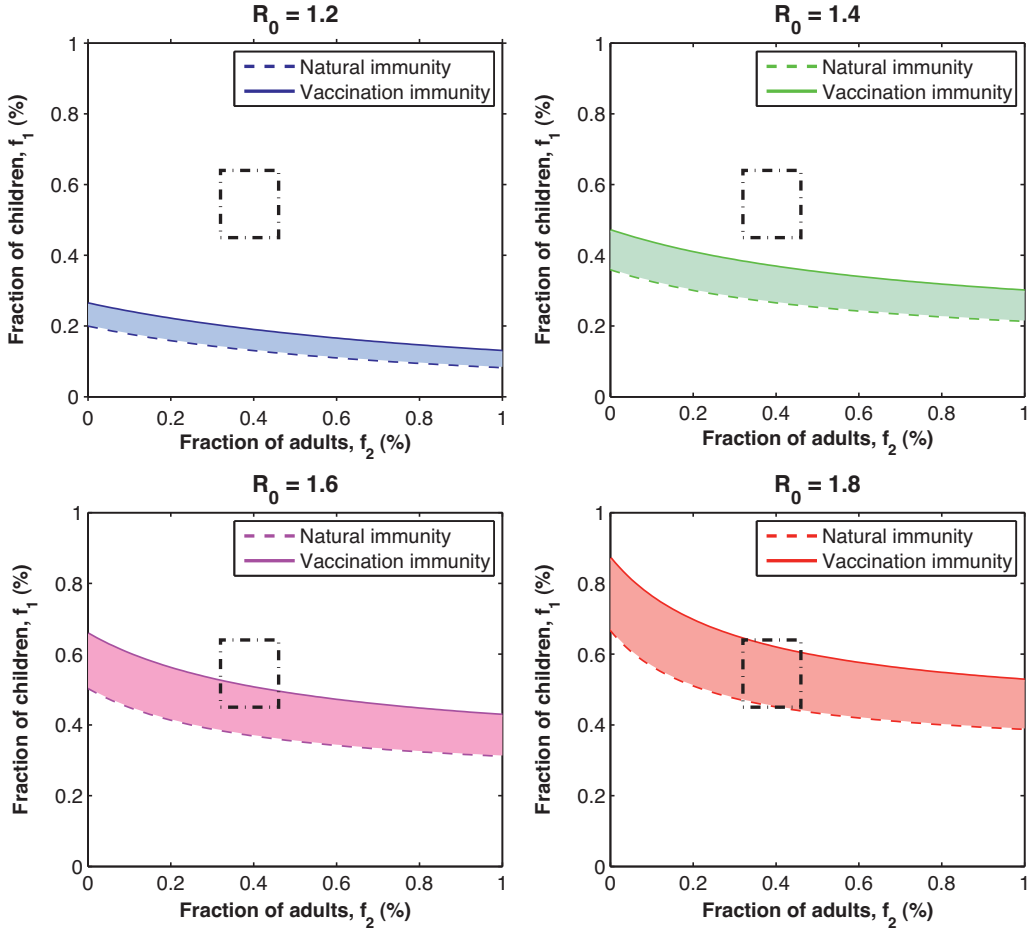

Fig. 4. The shaded regions indicate the *intermediate regions* for a specific R_0 (where $R_0 \in [1.2, 1.8]$) that is, the region where the threshold for a mixture of vaccine-induced immunity and natural immunity should lie. The level of combined immunity (vaccine-induced and naturally acquired immunity) at the end of winter 2010, calculated from on Centers for Disease Control and Prevention (2010a) and Ross et al. (2010), is given by the dotted square S.

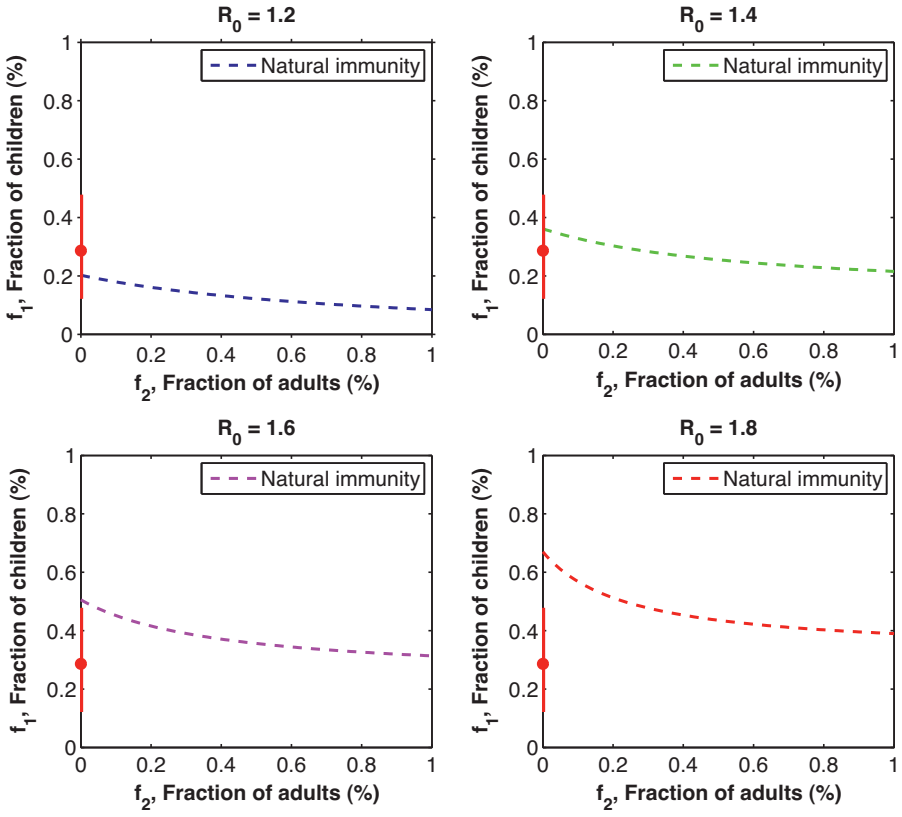

Fig. 5. Analysis for the second wave of pandemic H1N1 influenza in London and the West Midlands. The red mark and confidence intervals represent the fraction of children and adults naturally immune (people who became infected and recovered) by the end of the first wave. (For interpretation of the references to color in this figure legend, the reader is referred to the web version of this article.)

protected for the next wave. However, we do not precisely know the number of children who were infected during the first and second waves of pandemic H1N1 (spring and fall of 2009) nor the number of children who were vaccinated during the second wave (fall 2009). Moreover, we cannot guarantee that children who were vaccinated were not already immune, especially given the fact that a fraction of the infected children never develop symptoms. Therefore, we know that the level of protection of children should lie somewhere between $x\%$ and $(x+y)\%$. A similar analysis can be done for the adult age group.

We used this argument to estimate the level of combined immunity in children and adults in the winter 2010. First, we obtained raw estimates for the total number of people vaccinated and infected by using the information provided by the CDC (Centers for Disease Control and Prevention, 2010a). Then, we used the data given by Ross et al. (2010) to calculate the age-specific infection attack rates in children and adults by computing a weighted average of their estimates, where the weights were given by the proportions of the population in each age group according to US census data (U.S. Census Bureau, 2009). We assumed that vaccination was carried out independently of whether a person was previously infected or not. We considered the full range of estimates given by the CDC in Centers for Disease Control and Prevention (2010a), hence obtaining a rectangle S in the f_1f_2-plane of estimates of combined immunity at the end of winter 2009–2010 for children and adults, shown as a dotted box in Fig. 4. The center of this rectangle, corresponding to the mean of the estimates, gives the combined immune and vaccinated fraction of children to be about 54% and for adults to be about 37%.

Predicting the absence of a third wave of pandemic H1N1

Given an estimate for the level of combined immunity in winter 2010, we were able to correctly predict the absence of a third wave of pandemic H1N1. To do this, we looked at the estimated level of combined immunity together with the intermediate regions. The results are shown in Fig. 4. Provided that the rectangle S lies on or above the intermediate regions, the effective reproduction numbers will be below one and there will be no further transmission. The rectangle S lies above the intermediate regions for $R_0 = 1.2$, and $R_0 = 1.4$. According to our model, this implies that a third epidemic wave would not have occurred for these reproduction numbers. However, for $R_0 = 1.6$, the rectangle S overlaps with the intermediate region, and our model suggests that a third wave would have been possible. Finally, if the original R_0 were 1.8 or higher, our results suggest that substantial spread would have been possible.

There was no third wave of pandemic influenza in the US during the winter of 2010. Considering that most of the estimates for R_0 for pandemic H1N1 place it at 1.6 or below (Bacaer and Ait Dads, 2011; Fraser et al., 2009; Munayco et al., 2009; Pourbohloul et al., 2009; Tuite et al., 2010; White et al., 2009; Yang et al., 2009), our method correctly predicted the absence of this new epidemic wave.

Second wave in London and the West Midlands

For comparison, we present in this section an analogous analysis for the second wave of pandemic H1N1 influenza in London and the West Midlands, UK. Contrary to the US, the UK and in particular, England, experienced a big first epidemic wave of pandemic H1N1 influenza during the summer of 2009 (Health Protection Agency, 2009). This provides a unique opportunity for us to investigate

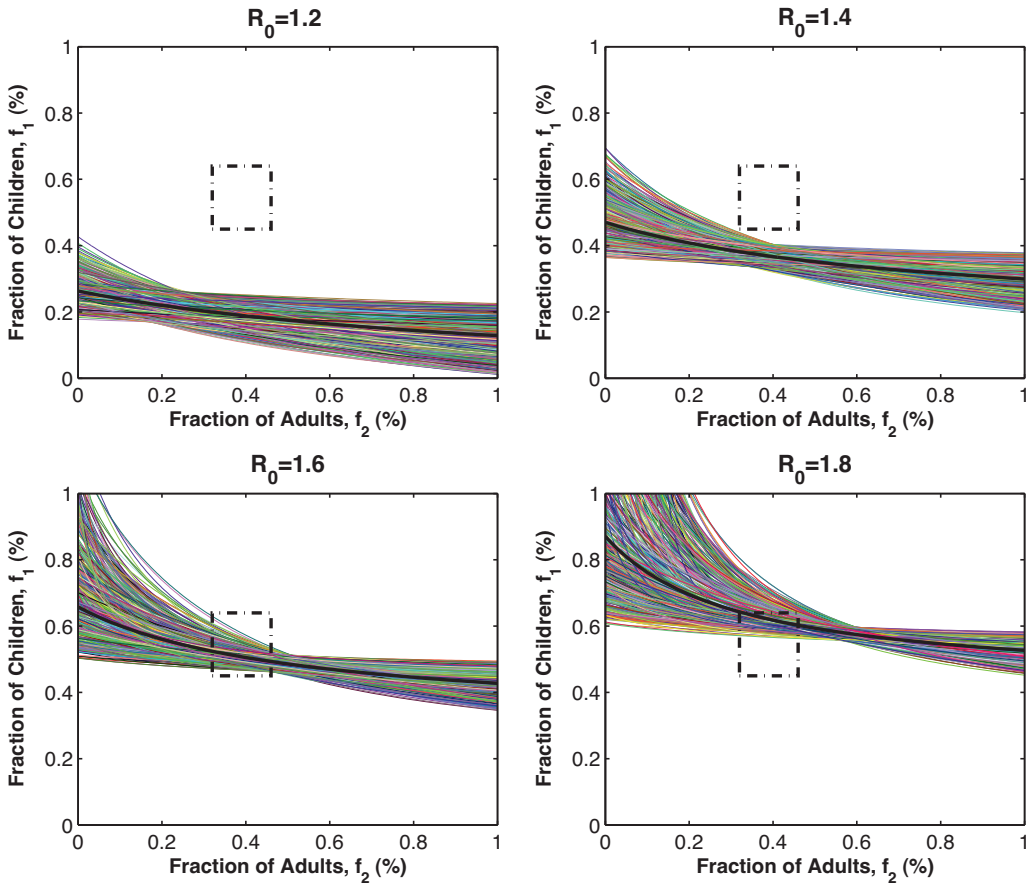

Fig. 6. Sensitivity analysis for the contact rates. For each run, the values of the contact rates were taken from a uniform distribution of length 0.2, centered at the value of the c_{ij} used. The contact rates were taken independently but only the triplets that gave $1.15 < R_0 < 1.25$, or $1.35 < R_0 < 1.45$, or $1.55 < R_0 < 1.65$ or $1.75 < R_0 < 1.85$ and where $c_{11} > c_{12}$ and $c_{11} > c_{22}$ were considered. The results are generally robust under this sensitivity. As long as $R_0 < 1.6$, all the runs lie below the dotted rectangle, indicating that a recurrent epidemic wave is very unlikely. For $R_0 = 1.6$, most of the curves intersect the rectangle, suggesting that a following wave is plausible. For $R_0 = 1.8$ most of the curves overlap with the rectangle or lie above the rectangle, indicating that a third wave would be very likely. The black curve indicates the critical vaccination curve used in the analysis.

whether our method can predict the occurrence of the second wave of pandemic H1N1 influenza in the fall of 2009, in the UK.

The main parameters of the model calibrated for the US epidemic do not change for the epidemic in England (contact rates, vaccine efficacies, etc.), so we only adjusted the proportion of children and adults in the population so that they matched the proportions in the UK. Since vaccine was introduced in the UK during the second wave, we only need to consider natural immunity, acquired through infection during the first wave (spring-summer 2009). We used the data for London and the West Midlands of Miller et al. (2010) to estimate the fraction of the children and the adults who became infected during the first wave in this region. Miller et al. (2010) partitioned the population into eight age groups (0–4, 5–14, 15–24, 25–44, 45–64, 65–74, 75–79, and ≥80 years), so we considered children to be up to 24 years old. The fraction of children previously infected was computed as a weighted average, where the weights corresponded to the proportion of the population in each age group in the UK (U.S. Census Bureau, 2011). We considered the full range of estimates given in Miller et al. (2010). In their paper, they found that there was no difference between the baseline (before the first wave of pandemic H1N1) and September 2009 for people in the older age groups (25 years and older). We then assumed that there were no adults immune after the first wave of H1N1 in London and the West Midlands.

The results are presented in Fig. 5. The estimate of the natural immunity in the children population in London and the West Midlands is shown in red. For $R_0 = 1.2$, the estimate for the natural immunity lies above the critical immune curve. Our method would then predict no further transmission. For $R_0 \geq 1.4$, the estimate lies below the critical immune curve, indicating that a new epidemic wave would be possible. We acknowledge that the assumption that no adults were infected during the first wave is unrealistic, but it is important to note that our method accurately predicts the second epidemic wave for $R_0 \geq 1.6$, for all possible values of natural immunity in the adult population. If $R_0 = 1.4$, then as long as less than 30% of the adults were infected during the first wave, our method predicts a new epidemic wave (see panel 2 Fig. 5). Given that most of the estimates for R_0 for pandemic H1N1 place it above 1.2, our results accurately predicted the second wave of pandemic H1N1 influenza in London and the West Midlands during the fall of 2009.

Sensitivity analysis

We performed a one-way sensitivity analysis for each of the contact rates, for the recovery rates in children and adults and for each of the vaccine efficacy parameters. Since $c_{12} = c_{21}$, we performed sensitivity analysis for the contact rates c_{11}, c_{12}, and c_{22} only. We drew values from a uniform distribution of length 0.2 centered around each value for the given contact rate. Each contact rate was drawn independently but only the triplets $\{c_{11}, c_{12}, c_{22}\}$ that satisfy the following conditions were chosen:

- The basic reproduction number obtained by using the contact rates fell into one of the following intervals: $1.15 < R_0 < 1.25$ or $1.35 < R_0 < 1.45$ or $1.55 < R_0 < 1.65$ or $1.75 < R_0 < 1.85$.

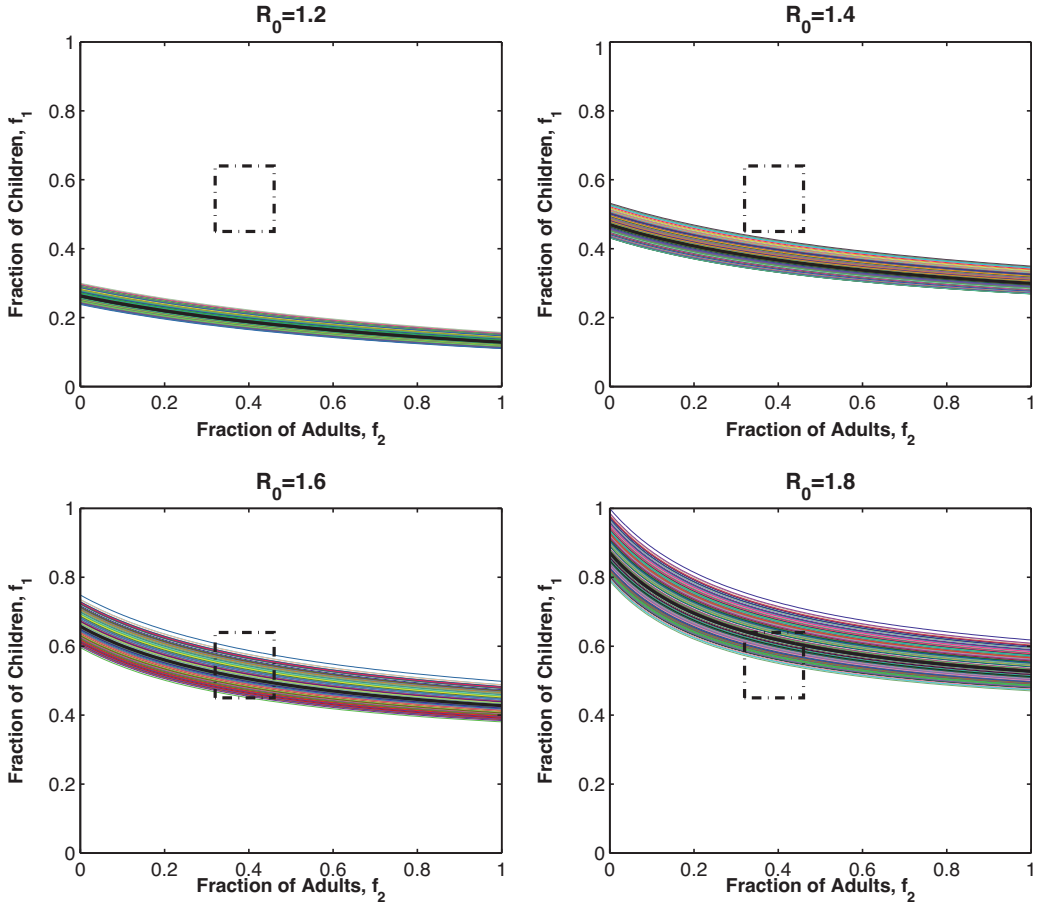

Fig. 7. Sensitivity analysis for the vaccine efficacies considered. The vaccine efficacies were taken from a uniform distribution of length 0.2 centered around the values used. Each vaccine efficacy was drawn independently. The results are quite robust with respect to these parameters.

- $c_{11} > c_{12}$ and $c_{11} > c_{22}$ (there are more contacts among children than among adults and more than between children and adults).

The results for 500 runs for each reproduction number are shown in Fig. 6. The general trends are quite robust for this sensitivity; if $R_0 = 1.2$ or $R_0 = 1.4$, all of the critical vaccination curves lie below the rectangle S. If $R_0 = 1.6$ there is some overlap with S, and for $R_0 = 1.8$ the majority of the curves intersect or lie above S.

For the vaccine efficacies, we analyzed the uncertainty by drawing a random number from a uniform distribution of length 0.2 centered around the value used. For each R_0, we performed 500 runs. The results are shown in Fig. 7. The trends are very robust with respect to these parameters as well.

Finally, we performed sensitivity analysis for the recovery rates for children and adults. For each recovery rate, we drew a random number from a uniform distribution of length 0.2, centered around the value used. We used only those pairs of recovery rates for children and adults for which the basic reproduction number fell into one of the following intervals: $1.15 < R_0 < 1.25$ or $1.35 < R_0 < 1.45$ or $1.55 < R_0 < 1.65$ or $1.75 < R_0 < 1.85$. As shown in Fig. 8, the results are robust with respect to these parameters.

Discussion

The approach proposed here, using information derived from the next generation matrix, provides simple thresholds for the vaccine-induced protection and natural immunity needed to prevent further spread of influenza, once a wave has passed. This can be particularly useful in a situation where most of the parameters are difficult to determine accurately. Most of the time we only have ranges of possible values. For example, determining the number of people infected from reported influenza illness data is difficult, given that a fraction of infections are asymptomatic. In addition, serosurveys can be problematic because of cross reacting antibodies. We have incorporated information about both the naturally induced immunity and the vaccination induced immunity, and we have discussed a possible interpretation of this mixture of immunity and its relationship to the naturally induced immunity only and to the vaccine-induced immunity only. The thresholds proposed here can be calculated exactly and even if a closed form might not always be available, symbolic software can help us in interpreting and using this information. We parametrized our influenza model for the pandemic H1N1 and used estimates given by the US Centers for Disease Control and Prevention (CDC) (Centers for Disease Control and Prevention, 2010a) and serosurvey data (Ross et al., 2010) to estimate the level of combined immunity due to vaccination and previous infection in the United States at the end of the second wave of pandemic influenza H1N1 (Fall 2010). Our computations suggested that for this epidemic, a third wave in the United States was unlikely if the original R_0 was 1.4 or lower, plausible for the low estimates of mixed immunity if the original R_0 was 1.6, and likely if the original R_0 was 1.8 or higher. Our results accurately predicted the absence of a third wave of pandemic influenza in the United States during the winter of 2010. It is worth noting that these results are conservative. This is because the serosurvey data was taken during the epidemic and not at the end of it. Since individuals might take up to several weeks to seroconvert,

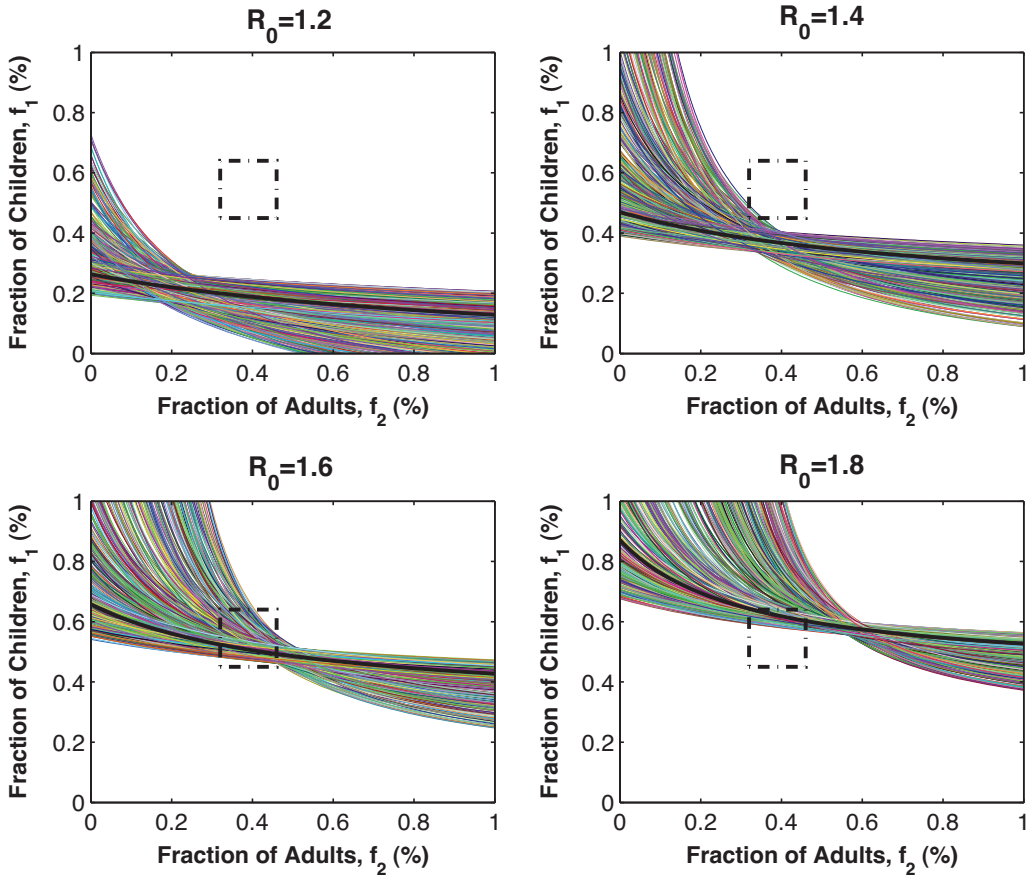

Fig. 8. Sensitivity analysis for the recovery rates for children and adults considered. Each recovery rate was independently taken from a uniform distribution of length 0.2 centered around the values used. Only those pairs for which the R_0 fell in one of the following intervals were used: $1.15 < R_0 < 1.25$, or $1.35 < R_0 < 1.45$, or $1.55 < R_0 < 1.65$ or $1.75 < R_0 < 1.85$. The results are very robust with respect to these parameters.

we most probably underestimated the level of immunity in the population. These results were used by the Los Angeles County, California, Department of Public Health as part of their response to the pandemic (Chao et al., 2011). Then, we repeated the analysis for predicting the second wave of pandemic H1N1 in London and the West Midlands. Using the estimates given in Miller et al. (2010), our method suggested that a second wave in London and the West Midlands was unlikely if $R_0 = 1.2$, but likely for all other values of R_0. This shows that our method accurately predicted the occurrence of the second wave of pandemic influenza in London and the West Midlands during the fall of 2009.

We used an influenza model capable of producing multiple epidemic waves. In order to make our results as general as possible, we used the simplest structure possible. In particular, we assumed that the probability of infection given contact was constant. Modifying this structure for specific situations would involve more complicated functions for the probability of infection, an interesting direction for future work. The approach proposed here has a number of limitations. First of all, this approach was based on either being able to explicitly find the largest eigenvalue in closed form or on graphically determining the largest eigenvalue of the next generation matrix. Obtaining closed forms for a more complicated system might be impossible, even with the help of symbolic software. While analyzing models with three age groups is still possible, working with more than three groups is impossible graphically and some other analytical technique would need to be employed. Also, the model proposed here is very simple. Even without changing the number of age groups, one can make it more realistic. For example, we could allow different probabilities of infection for children and adults or we could assume different recovery rates for asymptomatic and symptomatic individuals. Given that asymptomatic people will not reduce their level of activity, one could think of having different contact rates for the two infected groups. The approach used here to predict the recurrence of epidemic waves depends heavily on the next generation matrix, which in turn depends heavily in the contact pattern. Our sensitivity analysis showed that accurately estimating the contact rates is important. Our approach ignores the possibility that other factors, such as time-dependent contact rates, or the dates of school openings might predict new epidemic waves. We did not consider prior immunity to H1N1, which proved to be enough for protecting older populations (Centers for Disease Control and Prevention, 2010b). We did not consider future epidemic waves of H1N1. Finally, we did not take into account the possible antigenic drift of the virus that would make previous infected people again susceptible to some degree and would decrease vaccine efficacy. Incorporating this feature in our method would allow the possibility of investigating further H1N1 epidemics, like the ones that occurred in the UK and the rest of Europe during the winter of 2010–2011.

In the model of Hill and Longini (2003), the authors established thresholds for a model that does not include asymptomatics or vaccine efficacy for pathogenicity. In this sense, the current work is a natural extension of their model. The *SIR* model proposed here is similar to the one proposed by Brauer (2008), but we omitted the latent period and considered vaccination instead of treatment. They established useful final size relations and we established threshold conditions. Thus, these results complement each other. While our model was tailored for influenza, the methods used here can be

easily adapted for other acute infectious diseases. For example, this method could be applied to cholera. Cholera is an infectious disease with strong seasonality in some countries (Huq et al., 2005), and immunity due to natural infection and vaccines wane over a short period of time (Durham et al., 1998; Longini et al., 2002).

We believe that our approach is novel in that we were able to predict the occurrence (or not) of multiple epidemic waves by incorporating information of both the vaccine induced immunity and the naturally induced immunity. The method developed here suggests yet another effect of vaccination. Vaccination not only directly protects the vaccinated and indirectly protects the unvaccinated during the current wave, but it can also help in preventing subsequent waves of influenza.

Acknowledgments

This work was partially supported by National Institute of General Medical Sciences MIDAS grant U01-GM070749 and National Institute of Allergy and Infectious Diseases grant R01-AI32042.

The authors wish to thank two anonymous referees whose comments greatly improved the manuscript. LM was partially supported by Consejo Nacional de Ciencia y Tecnologia, Mexico, scholarship 196221. LM thanks Nicholas Cain for his help with the computational implementation of the method, Dennis Chao for providing the estimates used to plot the box in Fig. 4, Pauline van den Driessche for providing useful comments.

Appendix A.

Here, we give the details of the computation of the effective reproduction number used above. The code can be provided upon request. We use the approach given in Diekmann et al. (1990), Brauer et al. (2008) and van den Driessche and Watmough (2002). Let

$$\begin{array}{llllllll} S_{10}(0) & = \mathbf{S_{10}}, & S_{11}(0) & = \mathbf{S_{11}}, & S_{20}(0) & = \mathbf{S_{20}}, & S_{21}(0) & = \mathbf{S_{21}} \\ A_{10}(0) & = \mathbf{A_{10}}, & A_{11}(0) & = \mathbf{A_{11}}, & A_{20}(0) & = \mathbf{A_{20}}, & A_{21}(0) & = \mathbf{A_{21}} \\ I_{10}(0) & = \mathbf{I_{10}}, & I_{11}(0) & = \mathbf{I_{11}}, & I_{20}(0) & = \mathbf{I_{20}}, & I_{21}(0) & = \mathbf{I_{21}} \\ R_{10}(0) & = 0, & R_{11}(0) & = 0, & R_{20}(0) & = 0, & R_{21}(0) & = 0 \end{array}$$

be the initial conditions for the system (1)–(8) where

$$\mathbf{S_{10}} + \mathbf{S_{11}} + \mathbf{A_{10}} + \mathbf{A_{11}} + \mathbf{I_{10}} + \mathbf{I_{11}} = N_1,$$
$$\mathbf{S_{20}} + \mathbf{S_{21}} + \mathbf{A_{20}} + \mathbf{A_{21}} + \mathbf{I_{21}} + \mathbf{I_{21}} = N_2$$

and $\mathbf{A_{10}}, \mathbf{A_{11}}, \mathbf{I_{10}}, \mathbf{I_{11}}, \mathbf{A_{20}}, \mathbf{A_{21}}, \mathbf{I_{21}}, \mathbf{I_{21}}$ are very small positive numbers, each close to 0. Define

$$E_0 = (\mathbf{S_{10}}, \mathbf{S_{11}}, \mathbf{S_{20}}, \mathbf{S_{21}}, \mathbf{A_{10}}, \mathbf{A_{11}}, \mathbf{I_{10}}, \mathbf{I_{11}}, \mathbf{A_{20}}, \mathbf{A_{21}}, \mathbf{I_{21}}, \mathbf{I_{21}}, 0, 0, 0, 0).$$

If we set $\mathbf{A_{10}} = \mathbf{A_{11}} = \mathbf{I_{01}} = \mathbf{I_{11}} = \mathbf{A_{20}} = \mathbf{A_{21}} = \mathbf{I_{21}} = \mathbf{I_{21}} = 0$, and $\mathbf{S_{10}} + \mathbf{S_{11}} = N_1$, $\mathbf{S_{20}} + \mathbf{S_{21}} = N_2$ the model (1)–(8) has an infinite number of disease free equilibria, namely, one per each initial condition given. We linearize the system for the infectious equations (3)–(6) around the disease free equilibrium E_0. This gives us the matrices (as given in Brauer et al., 2008) F and V defined as follows.

$$F = pA \cdot \begin{pmatrix} \frac{c_{11}}{N_1}m & \frac{c_{12}}{N_2}m & \frac{c_{11}}{N_1}m\varphi & \frac{c_{12}}{N_2}m\varphi & \frac{c_{11}}{N_1} & \frac{c_{12}}{N_2} & \frac{c_{11}}{N_1}\varphi & \frac{c_{12}}{N_2}\varphi \\ \frac{c_{21}}{N_1}m & \frac{c_{22}}{N_2}m & \frac{c_{21}}{N_1}m\varphi & \frac{c_{22}}{N_2}m\varphi & \frac{c_{21}}{N_1} & \frac{c_{22}}{N_2} & \frac{c_{21}}{N_1}\varphi & \frac{c_{22}}{N_2}\varphi \\ \frac{c_{11}}{N_1}m & \frac{c_{12}}{N_2}m & \frac{c_{11}}{N_1}m\varphi & \frac{c_{12}}{N_2}m\varphi & \frac{c_{11}}{N_1} & \frac{c_{12}}{N_2} & \frac{c_{11}}{N_1}\varphi & \frac{c_{12}}{N_2}\varphi \\ \frac{c_{21}}{N_1}m & \frac{c_{22}}{N_2}m & \frac{c_{21}}{N_1}m\varphi & \frac{c_{22}}{N_2}m\varphi & \frac{c_{21}}{N_1} & \frac{c_{22}}{N_2} & \frac{c_{21}}{N_1}\varphi & \frac{c_{22}}{N_2}\varphi \\ \frac{c_{11}}{N_1}m & \frac{c_{12}}{N_2}m & \frac{c_{11}}{N_1}m\varphi & \frac{c_{12}}{N_2}m\varphi & \frac{c_{11}}{N_1} & \frac{c_{12}}{N_2} & \frac{c_{11}}{N_1}\varphi & \frac{c_{12}}{N_2}\varphi \\ \frac{c_{21}}{N_1}m & \frac{c_{22}}{N_2}m & \frac{c_{21}}{N_1}m\varphi & \frac{c_{22}}{N_2}m\varphi & \frac{c_{21}}{N_1} & \frac{c_{22}}{N_2} & \frac{c_{21}}{N_1}\varphi & \frac{c_{22}}{N_2}\varphi \\ \frac{c_{11}}{N_1}m & \frac{c_{12}}{N_2}m & \frac{c_{11}}{N_1}m\varphi & \frac{c_{12}}{N_2}m\varphi & \frac{c_{11}}{N_1} & \frac{c_{12}}{N_2} & \frac{c_{11}}{N_1}\varphi & \frac{c_{12}}{N_2}\varphi \\ \frac{c_{21}}{N_1}m & \frac{c_{22}}{N_2}m & \frac{c_{21}}{N_1}m\varphi & \frac{c_{22}}{N_2}m\varphi & \frac{c_{21}}{N_1} & \frac{c_{22}}{N_2} & \frac{c_{21}}{N_1}\varphi & \frac{c_{22}}{N_2}\varphi \end{pmatrix}$$

where A is given by

$$A = \text{diag}(S_{10}(1-\rho),\ S_{20}(1-\rho),\ S_{11}(1-\rho\psi)\theta, S_{21}(1-\rho\psi)\theta, S_{10}\rho,\ S_{20}\rho,\ S_{11}\rho\psi\theta,\ S_{21}\rho\psi\theta),$$

and V is given by

$$V = diag(\gamma_1, \gamma_2, \gamma_1, \gamma_2, \gamma_1, \gamma_2, \gamma_1, \gamma_2)$$

here $diag(a, \ldots, b)$ denotes a diagonal matrix with elements $a, \ldots, b$ on the diagonal. The matrix $K = FV^{-1}$ is called the next generation matrix. The effective reproduction number R_f is then given by

$$R_f = \rho(K)$$

where $\rho(K)$ is the spectral radius of K, that is, the largest eigenvalue of K in absolute value.

Recall that f_1 was defined to be the fraction of vaccinated children and f_2 was defined to be the fraction of vaccinated adults, where we assume that vaccination occurred prior to the beginning of the epidemic. If the number of initial infections is small, we have

$$\begin{array}{ll} \mathbf{S_{10}} \approx (1-f_1)N_1 & \mathbf{S_{11}} \approx f_1 N_1 \\ \mathbf{S_{20}} \approx (1-f_2)N_2 & \mathbf{S_{21}} \approx f_2 N_2. \end{array}$$

The matrix K for this particular model has rank 2, allowing us to conclude that the eigenvalue 0 has multiplicity 6 and that the remainder eigenvalues can be calculated as the root of the characteristic polynomial $P(\lambda)$ given by

$$\begin{aligned} P(\lambda) = \lambda^2 &+ \frac{1}{\gamma_1\gamma_2 N_1 N_2}(c_{11}\gamma_2 N_2 p(-\rho((1-f_1)N_1 + f_1 N_1 \phi\psi\theta) \\ &+ m((1-f_1)N_1(\rho-1) + f_1 N_1 \phi(\psi\rho - 1)\theta)) \\ &+ c_{22}\gamma_1 N_1 p(-\rho((1-f_2)N_2 + f_2 N_2 \phi\psi\theta) \\ &+ m((1-f_2)N_2(\rho-1) + f_2 N_2 \phi(\psi\rho-1)\theta)))\lambda \\ &+ \frac{1}{\gamma_1\gamma_2 N_1 N_2}(-c_{12}c_{21}p^2(-\rho((1-f_1)N_1 + f_1 N_1\phi\psi\theta) \\ &+ m((1-f_1)N_1(\rho-1) + f_1 N_1\phi(\psi\rho-1)\theta))(-\rho((1-f_2)N_2 \\ &+ f_2 N_2\phi\psi\theta) + m((1-f_2)N_2(\rho-1) + f_2 N_2\phi(\psi\rho-1)\theta)) \\ &+ c_{11}c_{22}p^2(-\rho((1-f_1)N_1 + f_1 N_1\phi\psi\theta) + m((1-f_1)N_1(\rho-1) \\ &+ f_1 N_1\phi(\psi\rho-1)\theta))(-\rho((1-f_2)N_2 + f_2 N_2\phi\psi\theta) \\ &+ m((1-f_2)N_2(\rho-1) + f_2 N_2\phi(\psi\rho-1)\theta))). \end{aligned}$$

The roots of $P(\lambda)$ were calculated to be

$$\begin{aligned} \lambda_{1,2} = \frac{1}{2\gamma_1\gamma_2 N_1 N_2}&\{c_{22}\gamma_1 N_1 N_2 p(f_2[m(1-\rho-\phi\theta+\rho\psi\theta) \\ &+ \rho(1-\phi\psi\theta)] - m - \rho + m\rho) \\ &+ c_{11}\gamma_2 N_1 N_2 p(f_1[m(1-\rho-\phi\theta+\phi\psi\rho\theta) + \rho(1-\phi\psi\theta)] - m \\ &- \rho + m\rho) \pm [p^2 4(c_{12}c_{21} - c_{11}c_{22})\gamma_1\gamma_2 N_1 N_2(-\rho N_1[(1-f_1) \\ &+ f_1\phi\psi\theta] + mN_1[(1-f_1)(\rho-1) + f_1\phi(\psi\rho-1)\theta]) \\ &\times(-\rho N_2[(1-f_2) + f_2\phi\psi\theta] + mN_2[(1-f_2)(\rho-1) \\ &+ f_2\phi(\psi\rho-1)\theta]) + (c_{11}\gamma_2 N_1 N_2[-\rho((1-f_1) + f_1\phi\psi\theta) \\ &+ m((1-f_1)(\rho-1) + f_1\phi(\psi\rho-1)\theta)] \\ &+ c_{22}\gamma_1 N_1 N_2[-\rho((1-f_2) + f_2\phi\psi\theta) + m((1-f_2)(\rho-1) \\ &+ f_2\phi\theta(\psi\rho-1))])^2]^{\frac{1}{2}}\}. \end{aligned} \tag{11}$$

The effective reproduction number R_f is the largest of these roots, i.e. the one with the positive sign in the square root.

References

Bacaer, N., Ait Dads, E., 2011. Genealogy with seasonality, the basic reproduction number, and the influenza pandemic. Journal of Mathematical Biology 62 (5), 741–762, doi:10.1007/s00285-010-0354-8.

Balcan, D., Hu, H., Goncalves, B., Bajardi, P., Poletto, C., Ramasco, J.J., Paolotti, D., Perra, N., Tizzoni, M., Van den Broeck, W., Colizza, V., Vespignani, A., 2009. Seasonal transmission potential and activity peaks of the new influenza A(H1N1): a Monte Carlo likelihood analysis based on human mobility. BMC Med 7, 45, doi:10.1186/1741-7015-7-45.

Barry, J.M., Viboud, C., Simonsen, L., 2008. Cross-protection between successive waves of the 1918–1919 influenza pandemic: epidemiological evidence from US Army Camps and from Britain. Journal of Infectious Diseases 198 (10), 1427–1434, doi:10.1086/592454.

Basta, N., Halloran, M.E., Matrajt, L., Longini, I.M., 2008. Estimating influenza vaccine efficacy from challenge and community-based study data. American Journal of Epidemiology 168 (12), 1343–1352.

Brauer, F., van den Driessche, P., Wu, J. (Eds.), 2008. Mathematical Epidemiology, vol. 1945 of Lecture Notes in Mathematics. Springer.

Brauer, F., 2008. Epidemic models with heterogeneous mixing and treatment. Bulletin of Mathematical Biology 70 (7), 1869–1885, doi:10.1007/s11538-008-9326-1.

Carrat, F., Vergu, E., Ferguson, N.M., Lemaitre, M., Cauchemez, S., Leach, S., Valleron, A.-J., 2008. Time lines of infection and disease in human influenza: a review of volunteer challenge studies. American Journal of Epidemiology 167 (7), 775–785, doi:10.1093/aje/kwm375.

Centers for Disease Control and Prevention, January 2010. CDC Estimates of 2009 H1N1 Influenza Cases, Hospitalizations and Deaths in the United States, April–December 12, 2009, http://www.cdc.gov/h1n1flu/estimates/April_December_12.htm?s_cid=cs_000, last accessed February 17th 2010.

Centers for Disease Control and Prevention, 2010, January. What You Should Know and Do this Flu Season If You Are 65 Years and Older, http://www.cdc.gov/h1n1flu/65andolder.htm, last accessed September 2011.

Chao, D.L., Matrajt, L., Basta, N.E., Sugimoto, J.D., Dean, B., Bagwell, D.A., Oiulfstad, B., Halloran, M.E., Longini, I.M.J., 2011. Planning for the control of pandemic influenza A (H1N1) in Los Angeles County and the United States. American Journal of Epidemiology 173 (10), 1121–1130, doi:10.1093/aje/kwq497.

Ciofi degli Atti, M.L., Merler, S., Rizzo, C., Ajelli, M., Massari, M., Manfredi, P., Furlanello, C., Scalia Tomba, G., Iannelli, M., 2008. Mitigation measures for pandemic influenza in Italy: an individual based model considering different scenarios. PLoS One 3 (3), e1790, doi:10.1371/journal.pone.0001790.

Diekmann, O., Heesterbeek, J., Metz, J., 1990. On the definition and computation of the basic reproduction ratio R0 in models for infectious-diseases in heterogeneous populations. Journal of Mathematical Biology 28 (4), 365–382.

Durham, L.K., Longini, I.M.J., Halloran, M.E., Clemens, J.D., Nizam, A., Rao, M., 1998. Estimation of vaccine efficacy in the presence of waning: application to cholera vaccines. American Journal of Epidemiology 147 (10), 948–959.

Fraser, C., Donnelly, C.A., Cauchemez, S., Hanage, W.P., Van Kerkhove, M.D., Hollingsworth, T.D., Griffin, J., Baggaley, R.F., Jenkins, H.E., Lyons, E.J., Jombart, T., Hinsley, W.R., Grassly, N.C., Balloux, F., Ghani, A.C., Ferguson, N.M., Rambaut, A., Pybus, O.G., Lopez-Gatell, H., Alpuche-Aranda, C.M., Chapela, I.B., Zavala, E.P., Guevara, D.M.E., Checchi, F., Garcia, E., Hugonnet, S., Roth, C., 2009. Pandemic potential of a strain of influenza A (H1N1): early findings. Science 324 (5934), 1557–1561, doi:10.1126/science.1176062.

Halloran, M.E., Struchiner, C.J., Longini, I.M., 1997. Study designs for evaluating different efficacy and effectiveness aspects of vaccines. American Journal of Epidemiology 146 (10), 789–803.

He, D., Dushoff, J., Day, T., Ma, J., Earn, D.J.D., 2011. Mechanistic modelling of the three waves of the 1918 influenza pandemic. Journal of Theoretical Ecology 2 (2), 283–288, doi:10.1007/s12080-011-0123-3.

Health Protection Agency, 2009. Weekly Epidemiological Updates Archive, http://www.hpa.org.uk/Topics/InfectiousDiseases/InfectionsAZ/PandemicInfluenza/H1N1PandemicArchive/SIEpidemiologicalData/SIEpidemiologicalReportsArchive/influswarchiveweeklyepireports/, last accessed September 2011.

Hill, A.N., Longini, I.M., 2003. The critical vaccination fraction for heterogeneous epidemic models. Mathematical Biosciences 181, 85–106, doi:10.1016/S0025-5564(02)00129-3.

Huq, A., Sack, R.B., Nizam, A., Longini, I.M., Nair, G.B., Ali, A., Morris, J.G.J., Khan, M.N.H., Siddique, A.K., Yunus, M., Albert, M.J., Sack, D.A., Colwell, R.R., 2005. Critical factors influencing the occurrence of Vibrio cholerae in the environment of Bangladesh. Applied and Environmental Microbiology 71 (8), 4645–4654, doi:10.1128/AEM.71.8.4645-4654.2005.

Longini, I.M., Ackerman, E., Elveback, L., 1978. Optimization model for influenza A epidemics. Mathematical Biosciences 38 (1–2), 141–157.

Longini, I.M., Sagatelian, K., Rida, W.N., Halloran, M.E., 1998. Optimal vaccine trial design when estimating vaccine efficacy for susceptibility and infectiousness from multiple populations. Statistics in Medicine 17, 1121–1136.

Longini, I.M.J., Yunus, M., Zaman, K., Siddique, A.K., Sack, R.B., Nizam, A., 2002. Epidemic and endemic cholera trends over a 33-year period in Bangladesh. Journal of Infectious Diseases 186 (2), 246–251, doi:10.1086/341206.

Longini, I.M.J., Halloran, M.E., Nizam, A., Yang, Y., 2004. Containing pandemic influenza with antiviral agents. American Journal of Epidemiology 159 (7), 623–633, doi:10.1093/aje/kwh092, arXiv:http://aje.oxfordjournals.org/cgi/reprint/159/7/623.pdf URL http://aje.oxfordjournals.org/cgi/content/abstract/159/7/623.

Lowen, A.C., Mubareka, S., Steel, J., Palese, P., 2007. Influenza virus transmission is dependent on relative humidity and temperature. PLoS Pathogens 3 (10), 1470–1476, doi:10.1371/journal.ppat.0030151.

Miller, E., Hoschler, K., Hardelid, P., Stanford, E., Andrews, N., Zambon, M., 2010. Incidence of 2009 pandemic influenza A H1N1 infection in England: a cross-sectional serological study. Lancet 375 (9720), 1100–1108, doi:10.1016/S0140-6736(09)62126-7.

Mossong, J., Hens, N., Jit, M., Beutels, P., Auranen, K., Mikolajczyk, R., Massari, M., Salmaso, S., Tomba, G.S., Wallinga, J., Heijne, J., Sadkowska-Todys, M., Rosinska, M., Edmunds, W.J., 2008. Social contacts and mixing patterns relevant to the spread of infectious diseases. PLoS Medicine 5 (3), 381–391, doi:10.1371/journal.pmed.0050074.

Munayco, C.V., Gomez, J., Laguna-Torres, V.A., Arrasco, J., Kochel, T.J., Fiestas, V., Garcia, J., Perez, J., Torres, I., Condori, F., Nishiura, H., Chowell, G., 2009. Epidemiological and transmissibility analysis of influenza A (H1N1)v in a southern hemisphere setting: Peru. Euro Surveillance 14 (32).

Olson, D., Simonsen, L., Edelson, P., Morse, S., 2005. Epidemiological evidence of an early wave of the 1918 influenza pandemic in New York City. Proceedings of the National Academy of Sciences of the United States of America 102 (31), 11059–11063, doi:10.1073/pnas.0408290102.

Pourbohloul, B., Ahued, A., Davoudi, B., Meza, R., Meyers, L.A., Skowronski, D.M., Villasenor, I., Galvan, F., Cravioto, P., Earn, D.J.D., Dushoff, J., Fisman, D., Edmunds, W.J., Hupert, N., Scarpino, S.V., Trujillo, J., Lutzow, M., Morales, J., Contreras, A., Chavez, C., Patrick, D.M., Brunham, R.C., 2009. Initial human transmission dynamics of the pandemic (H1N1) 2009 virus in North America. Influenza and Other Respiratory Viruses 3 (5), 215–222, doi:10.1111/j.1750-2659.2009.00100.x.

Ross, T., Zimmer, S., Burke, D., Crevar, C., Carter, D., Stark, J., Giles, B., Zimmerman, R., Ostroff, S., Lee, B., 2010. Seroprevalence following the second wave of pandemic 2009 H1N1 influenza. PLoS Current Influenza, RRN1148.

Schaffer, F.L., Soergel, M.E., Straube, D.C., 1976. Survival of airborne influenza virus: effects of propagating host, relative humidity, and composition of spray fluids. Archives of Virology 51 (4), 263–273.

Shaman, J., Pitzer, V.E., Viboud, C., Grenfell, B.T., Lipsitch, M., 2010. Absolute humidity and the seasonal onset of influenza in the continental United States. PLoS Biology 8 (2), e1000316, doi:10.1371/journal.pbio.1000316.

Soebiyanto, R.P., Adimi, F., Kiang, R.K., 2010. Modeling and predicting seasonal influenza transmission in warm regions using climatological parameters. PLoS One 5 (3), e9450, doi:10.1371/journal.pone.0009450.

Tuite, A.R., Greer, A.L., Whelan, M., Winter, A.-L., Lee, B., Yan, P., Wu, J., Moghadas, S., Buckeridge, D., Pourbohloul, B., Fisman, D.N., 2010. Estimated epidemiologic parameters and morbidity associated with pandemic H1N1 influenza. CMAJ 182 (2), 131–136, doi:10.1503/cmaj.091807.

U.S. Census Bureau, 2009. International Data Base, http://www.census.gov/population/international/data/idb/informationGateway.php, last accessed September 2011.

U.S. Census Bureau, 2009. Census 2000 Summary File 1, Matrices P13 and PCT12, http://www.census.gov/.

US Census Bureau, 2009. Fact Sheets, http://www.census.gov, last accessed November 24th, 2009.

van den Driessche, P., Watmough, J., 2002. Reproduction numbers and sub-threshold endemic equilibria for compartmental models of disease transmission. Mathematical Biosciences 180 (Special Issue), 29–48.

Wallinga, J., Teunis, P., Kretzschmar, M., 2006. Using data on social contacts to estimate age-specific transmission parameters for respiratory-spread infectious agents. American Journal of Epidemiology 164 (10), 936–944, doi:10.1093/aje/kwj317.

White, L.F., Wallinga, J., Finelli, L., Reed, C., Riley, S., Lipsitch, M., Pagano, M., 2009. Estimation of the reproductive number and the serial interval in early phase of the 2009 influenza A/H1N1 pandemic in the USA. Influenza and Other Respiratory Viruses 3 (6), 267–276, doi:10.1111/j.1750-2659.2009.00106.x.

WHO, 2009. Production and availability of pandemic influenza A (H1N1) vaccines, www.who.int/csr/disease/swineflu/frequently_asked_questions/vaccine_preparedness/production_availability/en/index.html, accessed July 28th, 2009.

Yang, Y., Sugimoto, J.D., Halloran, M.E., Basta, N.E., Chao, D.L., Matrajt, L., Potter, G., Kenah, E., Longini Jr., I.M., 2009. The transmissibility and control of pandemic influenza A (H1N1) virus. Science 326 (5953), 729–733, doi:10.1126/science.1177373.